Andrew T. Sullivan 109151173

Dynamic Causal Modeling Using fMRI and EEG

Introduction

Electroencephalography (EEG) signals are recorded on the surface of the scalp and are a result of large dendritic currents generated from quasisynchronous firing of large neuronal populations. This same underlying mechanism gives rise to local field potentials (LFPs), which have been shown to be a more reliable predictor of the blood oxygen level-dependent functional magnetic resonance imaging (BOLD-fMRI) signal than single- or multiunit recordings.[4] Summation of LFP currents over large distances produces the EEG response, and large signals generated far away from the recording electrode may also appear in the recorded signal in addition to local signals. The fMRI signal, conversely, is not a direct measure of neuronal activity, but rather measures the level of blood oxygenation, volume, and flow as a consequence of neural activity. Local activity in a region of the brain has been shown to result in increased oxygen levels, and thus a brighter fMRI signal.[3] This signal is a consequence of the paramagnetic properties of deoxyhemoglobin, which are not exhibited by its oxygenated counterpart. As the hemodynamic response to neural activity is complex, as evidenced by the presence of local oscillations without external stimulation, and the fact that it is truly measuring oxygen consumption, and thus metabolic activity, rather than directly measuring neuronal firing, it is necessary to uncover the relationship between the fMRI signal and underlying neuronal activity, as fMRI is a commonly used tool to assess activation of local brain regions.

The field of dynamic causal modeling (DCM) seeks to understand the links between signals such as fMRI and EEG, and has been used, for example, to investigate the link in cortical and subcortical networks during attention-based tasks.[7] It is beneficial to use EEG in conjunction with fMRI as both methods are noninvasive, may be recorded simultaneously, and the high temporal resolution of EEG compliments the high spatial resolution of MRI.[5]

Here, publicly available data is used in order to investigate the transfer function which couples the neural activity detected by EEG to the BOLD response recorded from fMRI. Though the data is largely preprocessed, SPM is used to obtain EEG intensity values, and corresponding voxels were estimated by eye to be used for a given EEG electrode. The System Identification toolbox in Matlab was used to evaluate the fit of numerous transfer functions to the experimental data. A single-electrode single-voxel response is compared to that averaged over the entire brain, with high levels of similarity between the waveforms.

Data Acquisition

The analyzed data was obtained from the OpenfMRI database, which contains publicly available imaging data. The “Auditory and Visual Oddball EEG-fMRI” dataset (accession number ds000116) was used in order to examine the relationship between neuronal electrical activity (EEG) and the hemodynamic response of the brain (fMRI).[2] The oddball task relies on the subject recognizing and responding to either an auditory or visual “oddball,” which occurs

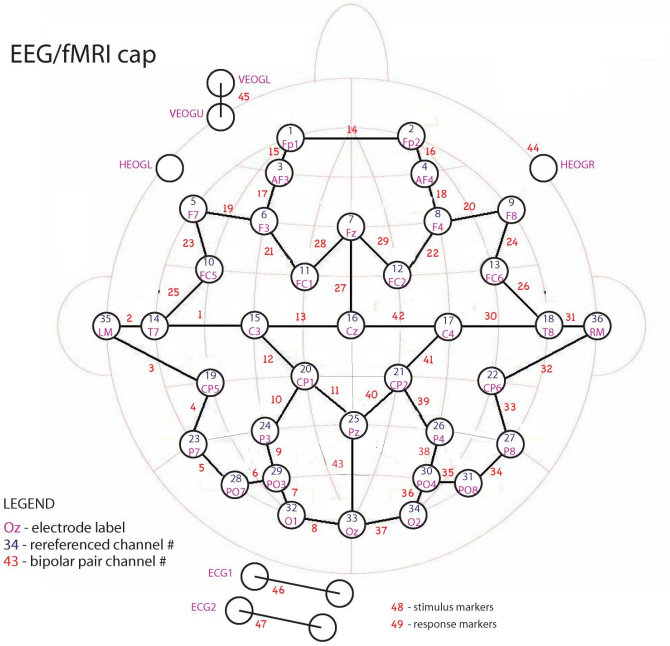

infrequently (20% of the stimuli for this dataset) and is characteristically different from the rest of the stimuli (i.e. a different color or tone). Within this dataset, the data from subject 1 was analyzed, in test 1 of run 1. This run examined auditory oddball data.

In order to properly correlate the electrical and hemodynamic responses, it is necessary to ensure that the analyzed data comes from the same area of the brain, i.e. that the data correspond to the same events. To do so, the EEG data from the trial was extracted and saved in the Matlab directory as a 49x340000 matrix, corresponding to the 49 electrode channels over the entire recording. The fMRI intensities for each voxel were extracted using the statistical parametric mapping (SPM) software package[6] and were saved in a 64x64x32x170 matrix within the Matlab workspace. The fMRI data was also opened in software which permitted identification of the specific voxels within the dataset. The EEG cap map displayed above was obtained in the supplementary data from the oddball dataset and was used to identify which time series in the dataset corresponds to which physical location on the scalp. It should be noted that the numbers on the electrode in the diagram are in "electrode space," while the data is presented using the numbers between the nodes. The value 16 was initially chosen due to this error, but was later changed to 27, which matched the fMRI activity more closely. The corresponding voxel matching this electrode was identified in the figure on the right, and has coordinates 31, 31, 29. Thus, the EEG activity from electrode dipole 27 was used in conjunction with the fMRI data from voxel 31, 31, 29 to estimate the transfer function between the two imaging modalities. Prior to comparison, the datasets had to be altered so that they were the same size. Thus, the number of EEG data points was reduced by taking the average of 2000 data points for each corresponding fMRI point. In other words, the first 2000 points were averaged and taken as point 1, the next 2000 as point 2, and so on. This ensured that the final datasets were the same size. This averaging is displayed in the figures below, which contains the fMRI voxel data along the top and the EEG data on the bottom, both before (left) and after (right) averaging. The presence of

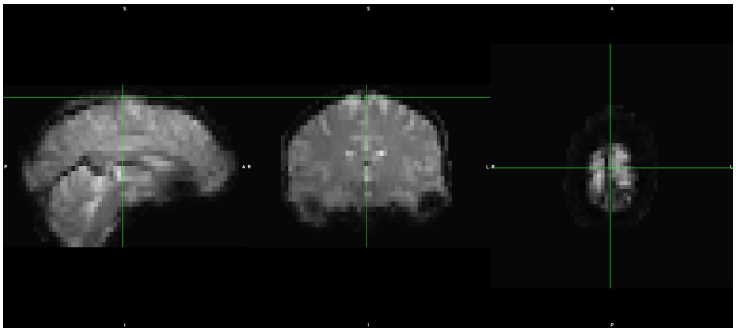

large peaks is approximately consistent between the two datasets, despite the averaging procedure.

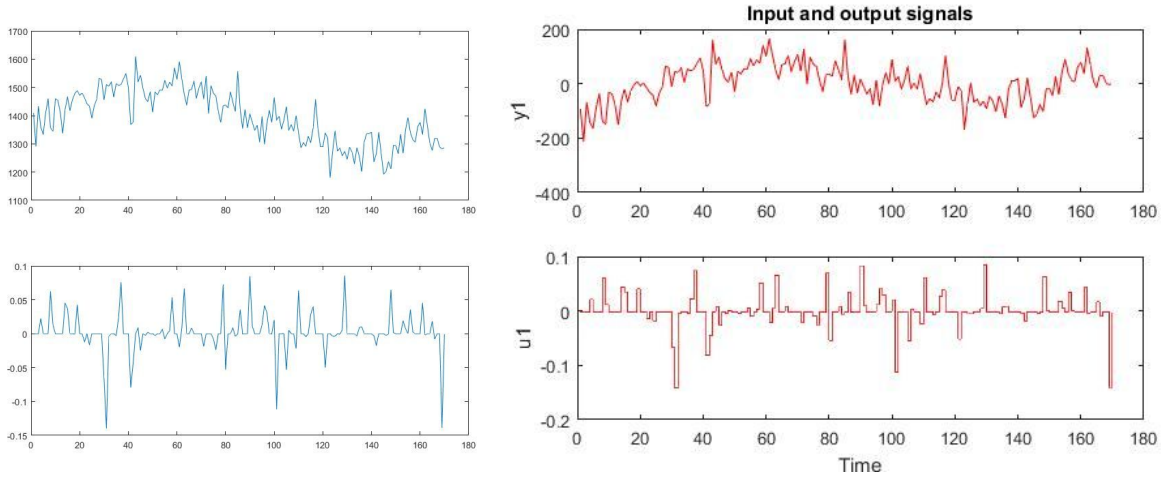

Data Analysis: Estimating the Transfer Function

The EEG-BOLD transfer function was estimated using the System Identification toolbox in Matlab. The inputs were taken to be the EEG data, corresponding to electrical activity of the brain, which cause the hemodynamic fMRI response, taken as the outputs. Both means and trends were removed from the data once imported, and the data was split in half into 85 data points for the estimation dataset and 85 data points for the validation dataset. Over 20 transfer functions were investigated in order to optimize both the fitting to the estimator set and the accuracy in predicting the validation set. However, maximum estimation fits were approximately 0.40, while those for validation were even lower (~0.30). It is likely that this is due to the large oscillations within the data, requiring transfer functions with large numbers of poles and zeros to reproduce. As an example, two of the best fits obtained are displayed to the left overlaid with the validation data. The gray curve fit the estimator data with an accuracy of only 24.07%, and the validation data with 16.57. This model consisted of 22 poles and 18 zeros. The red model, however, had a far better fit with the estimator data, at 42.43%, but only 4.866 with the validation data. As is evident from these results, the large oscillations in the EEG-fMRI relationship from only one electrode and one voxel require extremely complicated transfer functions.

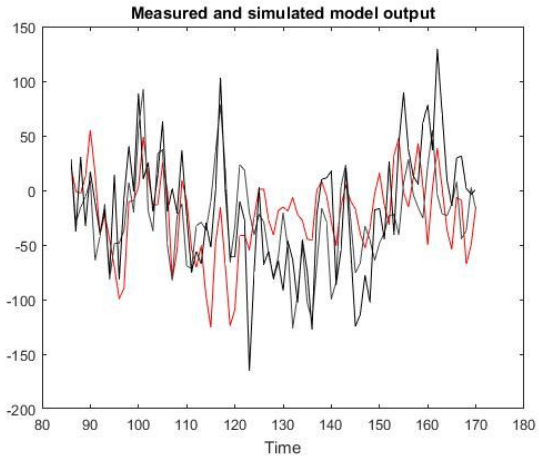

It is likely that the use of more data will result in transfer functions with far fewer poles and zeros and simpler functional forms, as the increased complexity of the functions is in part due to the presence of the oscillations. A procedure was used to obtain the average value over the entire brain, in order to investigate if including data from all EEG electrodes and all fMRI voxels could potentially smooth out the response curve. As is evident in the figure below, this is not the case. Comparison of the data averaged across all electrode channels and voxels for each time point and the data for the single channel-single voxel procedure reveals strong similarity between the datasets, and a transfer function of the form $(0.02786s+0.01759)/(s^2+0.08519s+0.001444)$ has a fit of 12.61 with the validation data, though the trend closely matches that of the data without the oscillations and of the simpler transfer function discussed above. Inspection of the EEG data for the single-channel and average recordings reveals noticeable differences in spikes of activity, though the fMRI data is far more similar. It should be noted that averaging across the entire dataset is not overly useful for a data obtained from the oddball task, as the purpose of the task is often to obtain differences in activity of specific brain regions, rather than over the entire brain. Thus, despite the similarities between the datasets, it is unlikely that this averaging would be used for proper analysis.

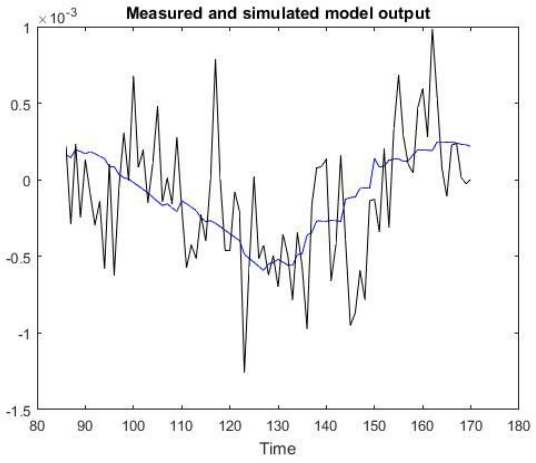

To account for regional activity, the average activity of each voxel from the fMRI data was determined, and the voxel with the maximum value was obtained. This voxel was found to be located in slice 25 at the position [45, 21]. Note that the "X," or first coordinate in the figure is the vertical axis, while the "Y" is the horizontal. The region is clearly evident in the image below, which depicts the average activity in slice 25. Though the location of this region along the X-Y axis of the figure is in the approximate location of auditory cortex, though not exactly overlapping with primary auditory cortex, viewing the voxel along the Z-axis reveals that this position is significantly more dorsal than auditory cortex. Instead, it is possible that this is an area of the posterior parietal cortex, which is implicated in integration of sensory information and in attention, the latter of which is likely to be a cause of activity in the oddball task. After many trials trying to find

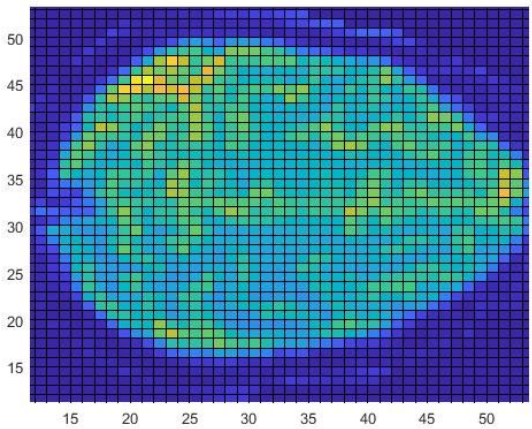

the optimal combination of voxels that will yield data consistent with the EEG electrodes, which were imported from the rereferenced data, containing the data from each actual electrode, rather than the bipolar pairs, the activity at each time point was averaged over a group of voxels coming from slices 24 and 25. The activity of 3 voxels for each slice were used in a given row. In slice 25, rows 44:47 were used, with columns 19:21 being used for row 44, and shifting one to the right for each subsequent row. A similar selection criterion was used for slice 24, including data from rows 44:48, and beginning with columns 17:19 in row 44. The resulting fMRI data was used in conjunction with data from electrode 19, which is close to the area of interest, judging by the map. These data series are depicted in the figure below, with EEG on top and fMRI on the bottom. Transfer functions were tested using the "transfer function models" and "polynomial models" functions within the System Identification toolbox. The best calculated transfer function came from the latter, having 36 poles with 10 numerator coefficients and a delay of 55. This polynomial fit the estimation data with a calculated fit of 73.28%, and the validation data with 41.66. Though this is still not an ideal fit value, it is significantly better than that using a single voxel. The final results are depicted in the figure below for both the estimation data (left) and the validation data (right).

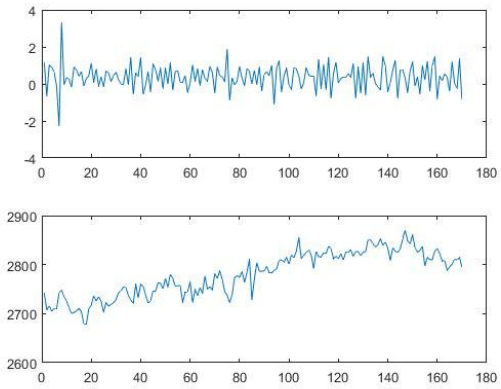

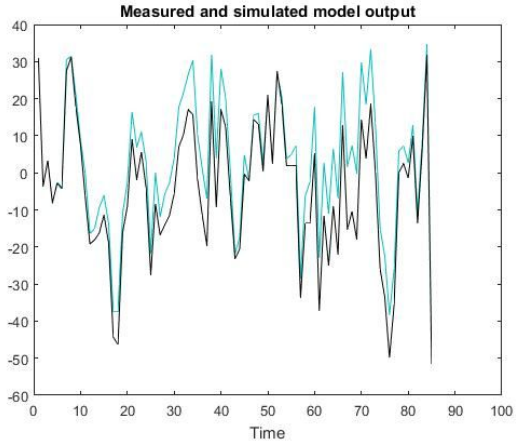

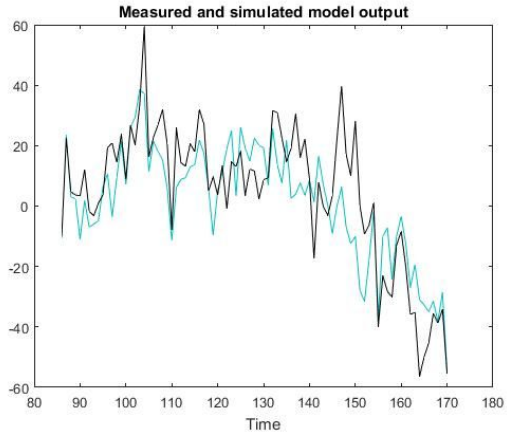

Conclusion: Improvements to Procedure

As evidenced by the relatively low fits of the above model, even for large numbers of poles and zeros in the transfer function, the methods used to analyze the above data are far from perfect. Numerous improvements can be made to the above procedures, and are often used in more advanced imaging paradigms with the availability of significantly larger computational power and available time. The most obvious improvement is a more quantifiable relationship between individual electrode signals and fMRI voxels. Other processing steps, such as the use of

a filter, may also be used to smooth this signal, as in [4]. This also may be a consequence of the low sample rate, which yielded only 170 data points, while the EEG obtained 2000 times more. This low sampling is bound to introduce error between the two signals, evidenced by the obvious noise between the two modalities, further exacerbating the oscillations of the response signals. Use of a sliding window or other means to preserve EEG data may be used. Other investigations of the EEG-fMRI transfer function have been performed with similar discrepancies, as they are a consequence of the imaging procedures themselves, but have also used complex methods to account for some of the other aforementioned issues, such as the need to average or downsample the EEG data prior to comparison with fMRI.[5] This lack of averaging prevents loss of EEG data in the form of short spikes, which may affect the resulting hemodynamic response.

Oscillations may also be smoothed with the introduction of more data. Within the oddball dataset, there were 17 subjects tested with two runs of three trials for each subject. Integrating this data into a larger dataset may also lead to better alignment between the data and the model. Bootstrapping algorithms may also be integrated by varying the chosen dataset for the estimation and validation procedures, in order to obtain statistical bounds on the obtained parameters.[1]

References

1. Conroy, Bryan R., Jennifer M. Walz, and Paul Sajda. “Fast Bootstrapping and Permutation Testing for Assessing Reproducibility and Interpretability of Multivariate fMRI Decoding Models.” Ed. Xia Wu. *PLoS ONE* 8.11 (2013): e79271. *PMC*. Web. 23 Mar. 2018.
2. Walz, J. M., et al. (2013). “Auditory and Visual Oddball EEG-fMRI.” *OpenfMRI* accession number ds000116.
3. Menon, V. and S. Crottaz-Herbette (2005). "Combined EEG and fMRI studies of human brain function." Int Rev Neurobiol 66: 291-321.
4. Rosa, M. J., et al. (2010). "Estimating the transfer function from neuronal activity to BOLD using simultaneous EEG-fMRI." NeuroImage 49(2): 1496-1509.
5. Sato, J. R., et al. (2010). "From EEG to BOLD: Brain mapping and estimating transfer functions in simultaneous EEG-fMRI acquisitions." NeuroImage 50(4): 1416-1426.
6. “Statistical Parametric Mapping.” *Wellcome Trust Centre for Neuroimaging*.
7. Walz, J. M., et al. (2013). "Simultaneous EEG-fMRI reveals temporal evolution of coupling between supramodal cortical attention networks and the brainstem." J Neurosci 33(49): 19212-19222.